Design of Polymer Electrolytes Based on a Lithium Salt of a Weakly Coordinating Anion to Realize High Ionic Conductivity with Fast Charge-Transfer Reaction

Hiroyuki Tokuda,[†,‡] **Sei-ichiro Tabata,**[†,‡] **Md. Abu Bin Hasan Susan,**[†,¶] **Kikuko Hayamizu,**[§] and **Masayoshi Watanabe*,**[†,‡]

Department of Chemistry and Biotechnology, Yokohama National University, 79-5 Tokiwadai, Hodogaya-ku, Yokohama 240-8501, Japan, Core Research for Evolutional Science and Technology, Japan Science and Technology Agency, and National Institute of Advanced Industrial Science and Technology, AIST Tsukuba Centre 5, Tsukuba 305-8565, Japan

Received: March 27, 2004; In Final Form: May 28, 2004

To design polymer electrolytes with high ionic conductivity as well as fast charge-transfer reaction at the electrode interface, electrolyte properties of a novel lithium salt of a weakly coordinating anion, lithium tetra(1,1,1,3,3,3-hexafluoro-2-propyl)aluminate, $LiAl[OCH(CF_3)_2]_4$, have been studied in the bulk, in aprotic solvents, and in a polyether. Although the lithium salt melts at fairly low temperature, it shows poor conductivity even in the molten state because of its strong ionic association. However, in aprotic solvents, $LiAl[OCH(CF_3)_2]_4$ exhibits a relatively high degree of dissociation because of weak coordination ability of the anion toward the cation. This is reflected in the higher ionic conductivity than that of common lithium salts, $LiN(SO_2CF_3)_2$ and $LiBF_4$, at an identical concentration in the low polar solvents. In a polyether, an increase in the glass-transition temperature (T_g) of the polymer electrolytes with salt concentration is less marked in the $LiAl[OCH(CF_3)_2]_4$ system. The lithium salt can be incorporated in the matrix polyether at high concentrations without a loss in the ionic conductivity. The interface between the polyether electrolyte containing $LiAl[OCH(CF_3)_2]_4$ and a metallic lithium electrode is statically stable for a long time, and the charge-transfer resistance decreases with increased salt concentration. These results indicate that an increase in $LiAl[OCH(CF_3)_2]_4$ concentration in the polyether facilitates not only an increase in the ionic conductivity but also a decrease in the interfacial resistance.

Introduction

The surge of interest in solid polymer electrolytes can be easily justified from their recognition as the most viable electrolytes for potential application in a wide variety of solid-state electrochemical devices and sensors. For their practical use in such devices, the resistances of the bulk polymer electrolytes and at the solid−solid interface between the polymer electrolytes and electrodes need to be indispensably low. This necessitates a proper and systematic understanding of the ion conduction mechanism in the electrolytes and of the rapid charge-transfer reaction at the electrode interface.

Most of the studies to date use poly(ethylene oxide) (PEO) and its derivatives as matrix polymers, and monomeric lithium salts are dissolved in the matrix polyether with a view to their direct application in rechargeable lithium metal anode batteries.[1−3] In the conventional polyether electrolytes, the ionic transport occurs cooperatively with segmental motion of the polyethers. This system is recognized as a "coupled system", where relaxation time for the segmental motion of the polymer host is close to the conduction relaxation time. Molecular design to achieve fast ion transport in such systems has been based on the preparation of polyethers having low-glass-transition temperatures (T_g)[4−6] and having hyperbranched structures to utilize fast molecular motion of the ion-coordinating side chains for the ionic transport.[7,8] Although these have been established to be effective means to increase ionic conductivity to some extent, the conductivity values at ambient temperature are still lower than those of common aprotic electrolyte solutions by about 2 orders of magnitude. The meager conductivity can partly be attributed to the fact that an increase in the number of carrier ions causes a serious decrease in the ionic mobility. While strong polyether−ion interaction assists the ionic dissociation and transport, it simultaneously suppresses the polymer dynamics, which is reflected in an increase in the T_g of the electrolytes.

The strategies to achieve highly ion conductive polymer electrolytes also include dissolving an electrolyte salt characterized by low T_g and/or melting point (T_m) with high ionic conductivity at room temperature in a compatible polymer. Typical examples are molten salts or room-temperature ionic liquids.[9−12] In the materials of this variety, also known as polymer-in-salt electrolytes, increase in the number of carrier ions and the ionic mobility are compatible with an increase in the electrolyte salt concentration. Some of the polymer-in-salt electrolytes behave as a "decoupled system", where the conduction relaxation time is decoupled from and is much faster than the structural relaxation time. This is because the self-ion-conducting salt plays an important role for the ionic conduction and a polymer matrix works as a rigid framework.[9,12] It is interesting to reveal the difference in ionic conduction mechanisms arising from the difference in electrolyte salt properties.

When a strongly electron-accepting lithium ion is fixed as a cationic species, the anionic design is only allowed for the

---

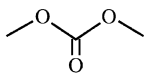* To whom correspondence should be addressed. Fax: +81-45-339-3955; e-mail: mwatanab@ynu.ac.jp.
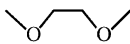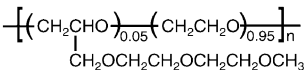† Yokohama National University.
‡ Japan Science and Technology Agency.
§ National Institute of Advanced Industrial Science and Technology.
¶ Permanent address: Department of Chemistry, University of Dhaka, Dhaka 1000, Bangladesh.

TABLE 1: Basic Properties of Solvents for Electrolyte Solutions and Polymer Electrolytes

Name	Structure	η / cP[a]	ε[a]	DN[a]/kcalmol^{-1}	$E_T(30)$[a]/kcalmol^{-1}
Dimethyl carbonate		0.63[c]	3.1[e]	15.1[c]	38.1
1,2-Dimethoxyethane		0.45[d]	7.20[f]	23.9[f]	35.2
γ-Butyrolactone		1.75[c]	39.1[b,c]	15.9[c]	44.3

Name	Structure	Molecular weight	T_g^g/°C	T_m^h/°C	Degree of crystallinity/%
P(EO/MEEGE)	$+\left[\left(CH_2CHO\right)_{0.05}\left(CH_2CH_2O\right)_{0.95}\right]_n+$ $\quad\quad\quad\vert$ $CH_2OCH_2CH_2OCH_2CH_2OCH_3$	$> 4.0 \times 10^6$ [i]	-61 [i]	47 [i]	38 [i]

$^a\eta$ (viscosity), ε (dielectric constant), DN (donor number), and $E_T(30)$ are the data at 25 °C. ^{b}At 20 °C. ^{c}Reference 34. ^{d}Reference 35. ^{e}Reference 36. ^{f}Reference 37. ^{g}Glass−transition temperature. ^{h}Melting point. ^{i}Reference 8a.

lithium salts. One may refer to the anionic structures of highly dissociable lithium salts in aprotic solvents for the design. The most common way to promote the dissociation in the aprotic media is the introduction of many electron-withdrawing groups, especially groups consisting of electronegative fluorine atoms, onto the anionic charge center. Highly charge-delocalized PF_6^- and $N(SO_2CF_3)_2^-$ are prime examples of the counteranion with relatively low ionic association, high conductivity, and electrochemical stability in aprotic media.[13-16] The design of an anionic species for weak coordination with a highly electrophilic cation has also received considerable attention in the fields of metallocene-catalyzed olefin polymerization, lithium-catalyzed Diels−Alder reactions, and 1,4-conjugate addition reactions to enhance the catalytic activity of metal cations. Fluorinated arylboranes, perfluoroborates, perfluoroaluminates, and halogenated carborane such as $CB_{11}H_{12-n}X_n^-$ (X = F, Cl, and I) are typical examples of a new class of weakly coordinating anions or superweak anions (the term has conceptually been introduced for a conjugate base of a superacid by S. H. Strauss) in the catalytic reaction field,[17,18] and some of these anions also seem to be directly applicable for electrochemical systems.[19,20]

In this study, to explore polymer electrolytes with high ionic conductivity and low interfacial resistance at the electrode interface, we have used lithium tetra(1,1,1,3,3,3-hexafluoro-2-propyl)aluminate, LiAl[OCH(CF$_3$)$_2$]$_4$, a lithium salt of a weakly coordinating anion. Electrolyte properties of the novel lithium salt have been studied in the bulk, in aprotic solvents, and in a polyether. A comparison with conventional lithium salts, LiBF$_4$ and LiN(SO$_2$CF$_3$)$_2$, has been made to investigate the anionic effect on the ion-transport properties in the aprotic solvents and polyether. In addition, we provide an insight into the interfacial charge-transfer properties and propose a strategy to control the charge-transfer reaction, in relation with the bulk properties of the polyether electrolytes.

There have been only few studies that correlate the charge-transfer reactions at the interface between a polyether electrolyte and metallic lithium with the bulk electrolyte properties.[21] It is demonstrated in this study that an increase in the glass-transition temperature (T_g) of the polyether electrolytes with salt concentration is less marked in LiAl[OCH(CF$_3$)$_2$]$_4$, which allows higher ionic conductivity at a higher salt concentration. The interfacial charge-transfer rate becomes higher with increased activity of

the lithium ion in the polyether electrolytes. The increase in the lithium salt concentration thus facilitates not only an increase in the ionic conductivity but also a decrease in the interfacial resistance.

Experimental Section

Materials and Preparation of Samples. LiAl[OCH(CF$_3$)$_2$]$_4$, generously supplied by Central Glass Co. Ltd., was used as received. LiBF$_4$ (Tomiyama Pure Chemical Industries Ltd.) and LiN(SO$_2$CF$_3$)$_2$, kindly supplied by Morita Chemical Industries Co. Ltd., were dried under high vacuum at 150 °C for 48 h. All of the lithium salts were stored in an argon atmosphere glovebox (VAC, [O$_2$] < 1 ppm, [H$_2$O] < 1 ppm). Lithium battery grade 1,2-dimethoxyethane (DME), dimethyl carbonate (DMC), and γ-butyrolactone (GBL) were purchased from Kishida Chemical Co. Ltd. and used without further purification. A high molecular weight polyether comb polymer, poly[ethylene oxide-*co*-2-(2-methoxyethoxy)ethyl glycidyl ether], P(EO/MEEGE) (kindly supplied by Daiso Co. Ltd., structure shown in Table 1), was used as a matrix of solid polymer electrolytes, and prior to use, was dried under high vacuum at 50 °C for 72 h and stored in the glovebox.

All of the sample preparations were carried out in the glovebox. For electrolyte solutions, each of the lithium salts, maintaining the concentration of 0.5 mol kg^{-1}, was dissolved in DME, DMC, and GBL. For solid polymer electrolytes, given amounts of the lithium salts and P(EO/MEEGE) copolymer were dissolved in anhydrous acetonitrile (Wako) to form a highly viscous homogeneous solution, followed by casting the viscous solution on a poly(tetrafluoroethylene) (PTFE) plate. To ensure that the films obtained are homogeneous and flat, the solvent was allowed to undergo slow evaporation at room temperature in the glovebox for several hours and then under high vacuum for 48 h.

Thermal Analysis. Differential scanning calorimetry (DSC) was carried out on a Seiko Instruments DSC 220C under a nitrogen atmosphere. The samples were tightly sealed in Al pans in the dry glovebox. For LiAl[OCH(CF$_3$)$_2$]$_4$, the sample pan was heated to 130 °C and then cooled to a given temperature and then reheated at several scanning rates with the same cooling and heating rate in a cycle. For the solid polymer electrolytes,

Design of Polymer Electrolytes

J. Phys. Chem. B, Vol. 108, No. 32, 2004 **11997**

the samples were heated to 80 °C and cooled to −150 °C and then heated at a rate of 10 K min^{-1}. The DSC thermograms in all the cases were recorded during the programmed reheating steps.

Electrochemical Measurements. The bulk ionic conductivity was measured by means of complex impedance measurements, using a computer-controlled Hewlett-Packard 4192A LF impedance analyzer over the frequency range from 5 Hz to 13 MHz with an ac amplitude of 1 V. For the investigation of the interfacial phenomena between metallic lithium and the polymer electrolytes, the measurements followed the same method with the exception of the ac amplitude, which was 10 mV in this case. For the bulk conductivity of LiAl[OCH(CF$_3$)$_2$]$_4$ and the conductivity of the electrolyte solutions, measurements were conducted using platinized platinum electrode cells (TOA Electronics, CG-511B) with the cell constants determined by a standard KCl aqueous solution. For the P(EO/MEEGE)-based polymer electrolytes, a film (0.2 mm thickness) was cut into disks of 10 mm diameter, and put into a PTFE ring spacer (13 mm o.d., 10 mm i.d., 0.2 mm thickness). The polymer electrolyte films with the PTFE ring spacers were sandwiched between mirror-finished stainless steel electrodes and were sealed in PTFE containers in the glovebox before they were subjected to the complex impedance measurements. For the interfacial measurement, the polymer electrolyte film with a polypropylene (PP) ring spacer (13 mm o.d., 10 mm i.d., 0.2 mm thickness), sandwiched between two symmetrical lithium electrodes (Honjo Metal Co.), was sealed in a PP container in the glovebox.

Self-Diffusion Coefficients. The pulse-gradient spin−echo NMR (PGSE-NMR) measurements were conducted by using a JEOL JNM-AL 400 spectrometer with a 9.4 T narrow bore superconducting magnet equipped with a JEOL pulse field gradient probe and a current amplifier providing gradient strength up to 15.5 Tm^{-1}. The samples were inserted into a 5 mm (o.d.) NMR microtube (BMS-005J, Shigemi, Tokyo) to a height of 5 mm in the glovebox. The details of the procedure for the PGSE-NMR measurements have been discussed earlier.[22−25] The self-diffusion coefficients were measured using a simple Hahn spin−echo (i.e., 90°-τ-180°-τ-acquisition)-based sequence incorporating a gradient pulse in each τ period. The free diffusion echo signal attenuation, E, is related to the experimental parameters by[26]

$$\ln(E) = \ln(S/S_{g=0}) = -\gamma^2 g^2 D \delta^2 (\Delta - \delta/3) \qquad (1)$$

where S is the spin−echo signal intensity, δ is the duration of the field gradient with magnitude g, γ is the gyromagnetic ratio, D is the self-diffusion coefficient, and Δ is the interval between two gradient pulses. The measurements of the diffusion coefficients of the solvent, lithium ion, and anion were made by ^{1}H, ^{7}Li, and ^{19}F NMR, respectively. Prior to the PGSE-NMR measurements, spin−lattice relaxation time (T_1) and spin−spin relaxation time (T_2) of each nucleus were also measured to determine a recycle delay between each transition (i.e., >5 T_1) and Δ in each case. The ^{7}Li diffusion measurements were limited to reasonably short Δ in bulk LiAl[OCH(CF$_3$)$_2$]$_4$ and in polymer electrolytes, because of the low sensitivity and short spin−spin relaxation time. Therefore, Δ value used for the bulk LiAl[OCH-(CF$_3$)$_2$]$_4$ and polyether electrolytes was fixed at 20 ms, while the value was 50 ms for electrolyte solutions. Under the condition of our measurements, plots of the attenuation of the intensity, that is, $\ln(S/S_{g=0})$ versus $\gamma^2 g^2 \delta^2 (\Delta - \delta/3)$, yielded straight lines, and the self-diffusion coefficient can, therefore, be derived easily from the slope of the resulting straight lines. The anion, Al[OCH(CF$_3$)$_2$]$_4^-$, has PGSE-NMR sensitive ^{1}H and
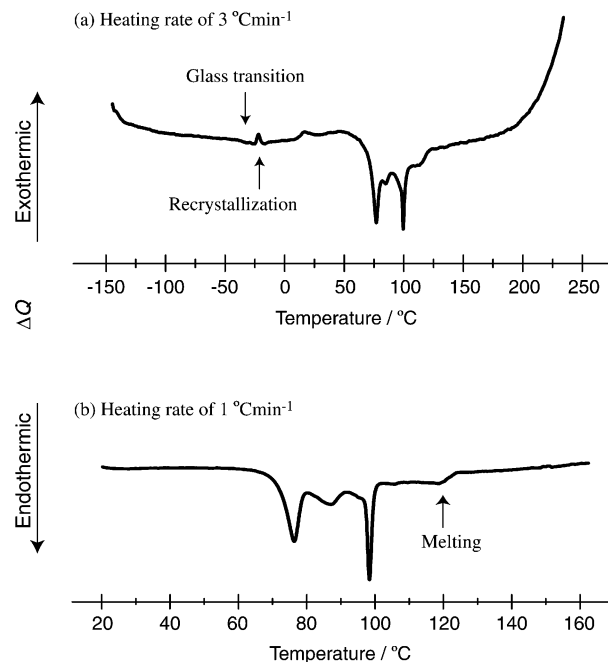

Figure 1. DSC thermograms of LiAl[OCH(CF$_3$)$_2$]$_4$ at a heating rate of 3 and 1 K min^{-1}.

^{19}F nuclei in the structure. The ^{1}H signals for the electrolyte solutions containing LiAl[OCH(CF$_3$)$_2$]$_4$ could be assigned for the solvent signals and the anion, respectively, and the self-diffusion coefficients could be independently estimated. The obtained ^{1}H and ^{19}F self-diffusion coefficients of the anion in the bulk LiAl[OCH(CF$_3$)$_2$]$_4$ and in the electrolyte solutions agree well with each other. However, the ^{1}H signal of the polyether electrolytes containing LiAl[OCH(CF$_3$)$_2$]$_4$ could not be separated for the short spin−spin relaxation time associated with it. The reliability of the obtained self-diffusion coefficients for bulk LiAl[OCH(CF$_3$)$_2$]$_4$ and some electrolyte solutions was cross-checked by replicate measurements by using a different system, a JEOL GSH-200 spectrometer with a 4.7 T wide-bore magnet controlled by TecMag Galaxy (subsequently the RF unit was replaced by a TecMag Apollo).[22−25]

Results and Discussion

Characterization of LiAl[OCH(CF$_3$)$_2$]$_4$. An aluminate anion, Al[OCH(CF$_3$)$_2$]$_4^-$, has high formula weight, and the crystallographic volume determined by X-ray diffraction is larger than that of typical counteranions.[13,27] The salt, LiAl-[OCH(CF$_3$)$_2$]$_4$, sublimes under high vacuum at an elevated temperature and is easily hydrolyzed when exposed to moisture, as is the case of LiPF$_6$. The thermal behavior also provides interesting characteristics of LiAl[OCH(CF$_3$)$_2$]$_4$. Figure 1 represents the DSC thermograms of LiAl[OCH(CF$_3$)$_2$]$_4$ at two different scan rates. The thermograms exhibit multiple peaks, especially in the temperature range from about 70 to 100 °C. The endothermic heat capacity change at −35 °C, followed by an exothermic peak, could be assigned to the T_g and the temperature of recrystallization, T_c, respectively. To identify the endothermic peak corresponding to the T_m and visualize the phenomenon behind the multiple peaks, we have used visual observation of the sample in a capillary with progressive heating. Upon heating from ambient temperature, the white solid LiAl-[OCH(CF$_3$)$_2$]$_4$ passes through a waxy state, and then completely fuses at about 120 °C. The final endothermic peak at 119 °C in the DSC thermogram can, therefore, be assigned to the T_m, which agrees well with the correlation of the T_g with the T_m,
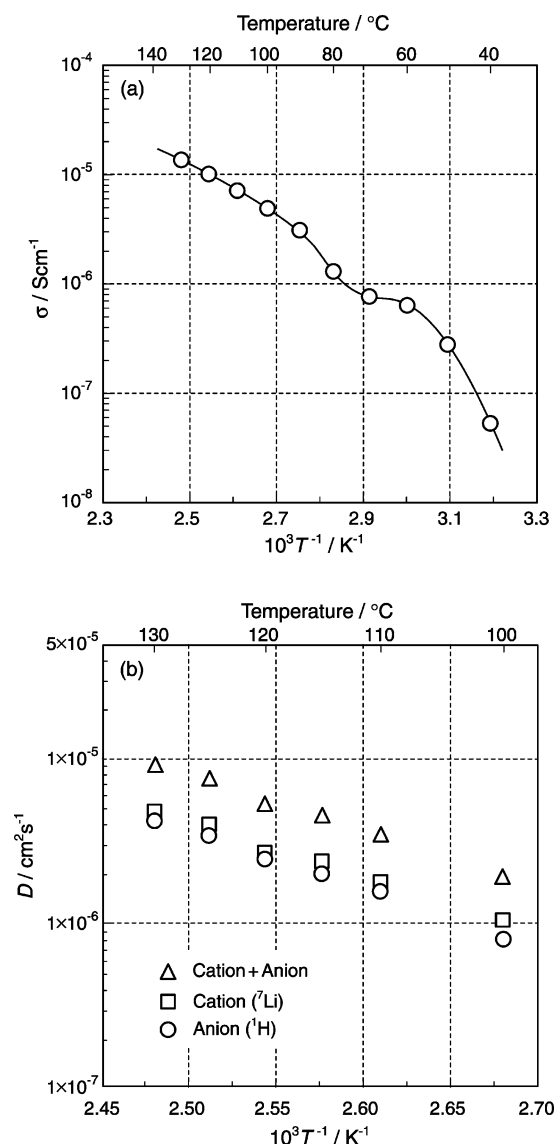
11998 *J. Phys. Chem. B, Vol. 108, No. 32, 2004*

Tokuda et al.

Figure 2. Arrhenius plots of (a) ionic conductivity and (b) self-diffusion coefficients of ^{7}Li, ^{19}F, and simple summation of ^{7}Li and ^{19}F for LiAl[OCH(CF$_3$)$_2$]$_4$ at a cooling scan.

TABLE 2: Ionic Conductivity, Self-Diffusion Coefficient, $\sigma_{imp}/\sigma_{diff}$ for DMC, DME, and GBL Based Electrolyte Solutions Containing LiBF$_4$, LiN(SO$_2$CF$_3$)$_2$, and LiAl[OCH(CF$_3$)$_2$]$_4$ at a Concentration of 0.5 mol kg^{-1} at 30 °C

| | | | $D/10^{-6}$ cm^2 s^{-1} | | | |
| | | $\sigma/10^{-3}$ | solvent | anion | cation | |
solvent	lithium salt	S cm^{-1}	(^{1}H)	(^{19}F)	(^{7}Li)	$\sigma_{imp}/\sigma_{diff}$
DMC	LiBF$_4$	0.058	20	7.8	8.0	0.0018
	LiN(SO$_2$CF$_3$)$_2$	2.1	16	6.1	6.0	0.085
	LiAl[OCH(CF$_3$)$_2$]$_4$	5.1	14	4.4	4.4	0.27
DME	LiBF$_4$	1.0	24	11	12	0.027
	LiN(SO$_2$CF$_3$)$_2$	8.0	24	12	11	0.20
	LiAl[OCH(CF$_3$)$_2$]$_4$	10	20	7.2	8.6	0.35
GBL	LiBF$_4$	7.1	5.9	4.1	2.6	0.50
	LiN(SO$_2$CF$_3$)$_2$	8.3	5.6	3.8	2.7	0.58
	LiAl[OCH(CF$_3$)$_2$]$_4$	5.2	5.4	2.2	2.1	0.52

apparent degree of dissociation roughly estimated by the conductivity ratio determined from impedance measurements and self-diffusion coefficients data using the modified Nernst−Einstein equation as described in the following section and also in the previous studies[14,28] has a value as low as 1.9×10^{-4}.

Xu et al. also reported that a fusible lithium salt, lithium bis-[1,2-tetra(trifluoromethyl) ethylenediolate (2-)-O,O'] borate, LiB[OC(CF$_3$)$_2$]$_4$,[29] with the characteristics similar to our system, has low T_m of 120 °C and low ionic conductivity of 7.1×10^{-6} S cm^{-1} at 120 °C. Both of the salts have analogous structures in the sense that there is great disparity between cationic and anionic size, which reflects low lattice energy as well as low T_m. The reported crystallographic structure, determined by X-ray diffraction, shows that LiAl[OCH(CF$_3$)$_2$]$_4$ consists of centrosymmetric dinuclear molecules of two lithium ions and two tetrahedral Al[OCH(CF$_3$)$_2$]$_4^-$.[27] The lithium ion is surrounded by oxygen and fluorine atoms from two different anionic substituents, −OCH(CF$_3$)$_2$. In the molten state, the strongly electrophilic lithium ion also seems to be trapped in its anionic cage formed by several electron-donating oxygen and fluorine atoms. Thus, LiAl[OCH(CF$_3$)$_2$]$_4$ has a covalent character which differs from that of the conventional ionic liquids.

Cyclic voltammetric measurements at a Ni working electrode with a Li reference and counter electrode have been used to evaluate the electrochemical stability of LiAl[OCH(CF$_3$)$_2$]$_4$ in ethylene carbonate (EC). The cyclic voltammogram clearly shows (data not shown) the deposition of metallic lithium at the cathodic limit and stripping of lithium in the reverse anodic scans. The irreversible oxidation in the reverse anodic scan is observed at ca. 5.2 V versus Li/Li$^+$ at the cutoff current density of 0.5 mA cm^{-2} in the first cycle of the measurement. Considering the stability of the Ni working electrode and EC, the lithium salt is stable at least 4.5 V versus Li/Li$^+$.

Electrolyte Solution Properties. Despite poor conductivity in the molten state, the lithium ion trapped by the anionic substituents may be released from the anionic cage by the introduction of basic solvents. The solution properties have been investigated by dissolving LiAl[OCH(CF$_3$)$_2$]$_4$ in some aprotic solvents with different polarity, and the solvent properties used in this study are listed in Table 1. Also, a comparison of the solution behavior has been made for common lithium salts, LiBF$_4$ and LiN(SO$_2$CF$_3$)$_2$. The ionic conductivity and self-diffusion coefficients of the solvent, lithium, and anion for nine electrolyte solutions at a concentration of 0.5 mol kg^{-1} at 30 °C are shown in Table 2.

The Nernst−Einstein equation correlates ionic conductivity with the ionic diffusion coefficient. Ionic conductivity of the electrolyte solution can be calculated from the self-diffusion

that is, $T_g/T_m = 2/3$ (the "2/3 rule"). Although a complete understanding of other small peaks is not available, the multiple peaks at temperature below the T_m and the small melting endothermic peak are similar to the behavior of plastic crystals. At a heating rate of 3 °C min^{-1}, a steep exothermic trace can be observed from about 200 °C in the DSC thermogram, which corresponds to the decomposition of LiAl[OCH(CF$_3$)$_2$]$_4$. The lithium aluminate salt is, therefore, thermally stable up to about 200 °C.

Figure 2 shows the Arrhenius plots of ionic conductivity and self-diffusion coefficients of the anion, Al[OCH(CF$_3$)$_2$]$_4^-$ (^{1}H), cation (^{7}Li), and the simple summation of the cation and anion (^{1}H and ^{7}Li) for the molten LiAl[OCH(CF$_3$)$_2$]$_4$ in a cooling scan. No inflection point for the conductivity and the self-diffusion coefficients at the T_m with decreasing temperature suggests that supercooling occurs in the lithium salt, which is further revealed by the DSC results. Despite the high self-diffusion coefficients of ^{7}Li and ^{1}H at 130 °C (4.8×10^{-6} and 4.3×10^{-6} cm^2 s^{-1}, respectively), the ionic conductivity of the molten salt at 130 °C is comparatively low (1.4×10^{-5} S cm^{-1}). The poor conductivity with high diffusivity may be ascribable to high ionic association in the molten LiAl[OCH(CF$_3$)$_2$]$_4$. In fact, the

coefficients, determined by the PGSE-NMR measurements, using the relationship

$$\sigma_{\mathrm{diff}} = \frac{Nq^2}{kT}(D_+ + D_-) \qquad (2)$$

where N is the number of charge carriers per cm^3 on the assumption of complete dissociation, q is the electric charge on each charge carrier, and D_+ and D_- are the diffusion coefficients of the cation and anion, respectively. It is possible to roughly estimate the degree of ionic dissociation from the ratio of the calculated conductivity value (σ_{diff}) and the value measured by complex impedance (σ_{imp}).[14,28] The calculated apparent degree of dissociation, $\sigma_{\mathrm{imp}}/\sigma_{\mathrm{diff}}$, is also listed in Table 2.

A close look at Table 2 reveals that in the relatively low polar solvents, DMC and DME, the $LiAl[OCH(CF_3)_2]_4$ solutions exhibit the highest conductivity, although the ionic diffusion coefficients are the lowest. The highest ionic conductivity of 1.0×10^{-2} S cm^{-1} at 30 °C is obtained for $LiAl[OCH(CF_3)_2]_4$ in DME. This is because the degree of dissociation, $\sigma_{\mathrm{imp}}/\sigma_{\mathrm{diff}}$, is considerably higher for the $LiAl[OCH(CF_3)_2]_4$ solutions than for other salt solutions, which seems to be caused by the relatively weak coordinating ability of $Al[OCH(CF_3)_2]_4^-$ toward the lithium cation. In the polar solvent, GBL, the difference in the degree of dissociation, $\sigma_{\mathrm{imp}}/\sigma_{\mathrm{diff}}$, is less pronounced depending on the anionic structures, and the order of the conductivity follows that of the diffusivity, which is determined by the anionic size as well as the solution viscosities. Since the solvation ability of GBL is high, the degree of dissociation does not depend on the coordinating ability of the anions.

Similar results to our findings, namely, the ionic conductivity being strongly dependent on the dissociation degree in low polar solvents, have also been reported by Webber[30] for $LiCF_3SO_3$ and $LiN(SO_2CF_3)_2$ solutions. The higher ionic conductivity despite the higher viscosity for the $LiN(SO_2CF_3)_2$ solutions has been explained by the difference in the anionic charge delocalization. The high dissociability of the aluminate salt in the low polar solvents is reflected by the weakly coordinating ability of the anion, which seems to be attained not only by the anionic charge delocalization but also by the steric hindrance effect of the bulky substituents.

Ionic Conductivity and T_g of Polymer Electrolytes. The significantly low T_g of the lithium salt along with the weak coordinating ability of the anion, as discussed in the preceding sections, makes $LiAl[OCH(CF_3)_2]_4$ an ideal choice for introduction in polyether matrixes. In this study, we used P(EO/MEEGE) copolymer as the matrix polyether for polymer electrolytes. The characteristics of the copolymer are shown in Table 1. Figure 3 shows temperature dependence of ionic conductivity for polymer electrolytes containing (a) $LiAl[OCH(CF_3)_2]_4$ at [Li]/[O] = 0.04−0.10 and (b) $LiBF_4$, $LiN(SO_2CF_3)_2$, and $LiAl[OCH(CF_3)_2]_4$ at [Li]/[O] = 0.10. It is evident from Figure 3a that an increase in $LiAl[OCH(CF_3)_2]_4$ concentration causes an increase in the ionic conductivity. Such an increase in conductivity could be observed till [Li]/[O] reaches the value of 0.10. Ionic conductivity of polyether-based electrolytes under such high salt concentration usually shows pronounced temperature dependency as can be seen in Figure 3b. However, the $LiAl[OCH(CF_3)_2]_4$ system has low apparent activation energy for the conductivity, compared to other lithium salts at an identical concentration.

Figure 4 shows ionic conductivity at 60 °C of the polyether electrolytes containing $LiBF_4$, $LiN(SO_2CF_3)_2$, and $LiAl[OCH(CF_3)_2]_4$ as a function of lithium salt concentration, while Figure

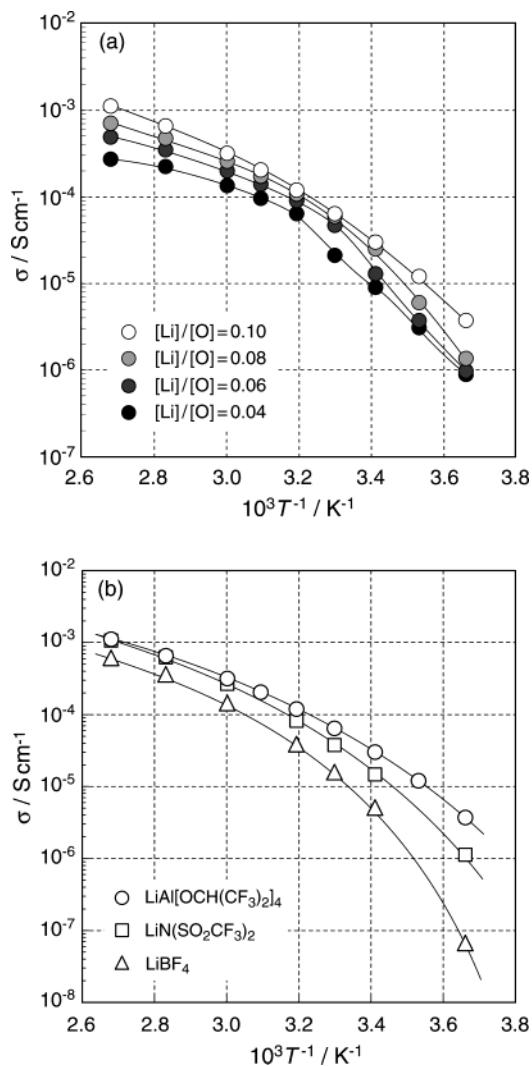**Figure 3.** Arrhenius plots of ionic conductivity for polymer electrolytes based on P(EO/MEEGE) = 95/5 containing (a) $LiAl[OCH(CF_3)_2]_4$ at different lithium salt concentrations and (b) $LiBF_4$, $LiN(SO_2CF_3)_2$, and $LiAl[OCH(CF_3)_2]_4$ at ([Li]/[O] = 0.10).

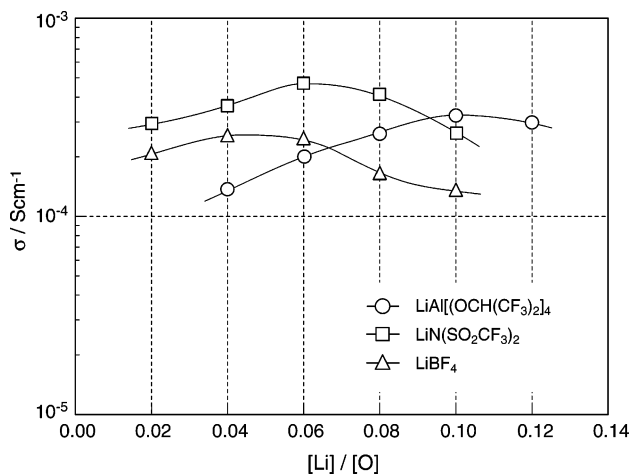**Figure 4.** Ionic conductivities of polymer electrolytes based on P(EO/MEEGE) = 95/5 containing $LiBF_4$, $LiN(SO_2CF_3)_2$, and $LiAl[OCH(CF_3)_2]_4$ as a function of salt concentration at 60 °C.

5 shows the T_g of the corresponding electrolytes. At a constant temperature, the conductivity increases with an increase in salt concentration and passes through a maximum before it starts to decrease with further increase in salt concentrations. As the
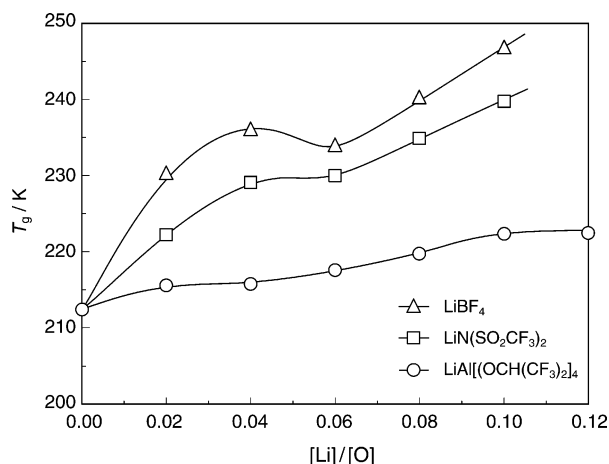
12000 *J. Phys. Chem. B, Vol. 108, No. 32, 2004*

Tokuda et al.

Figure 5. Glass-transition temperatures (T_g) of polymer electrolytes based on P(EO/MEEGE) = 95/5 containing LiBF$_4$, LiN(SO$_2$CF$_3$)$_2$, and LiAl[OCH(CF$_3$)$_2$]$_4$ as a function of salt concentration.

TABLE 3: Ionic Conductivity and Self-Diffusion Coefficients of Anion, Lithium Ion, and Simple Summation of Lithium Ion and Anion for P(EO/MEEGE) Based Polymer Electrolytes Containing LiBF$_4$, LiN(SO$_2$CF$_3$)$_2$, and LiAl[(OCH(CF$_3$)$_2$]$_4$ ([Li]/[O] = 0.10) at 80 °C

| | | $D/10^{-8}$ cm^2 s^{-1} | | |
| | | anion | cation | total |
lithium salt	$\sigma/10^{-4}$ S cm^{-1}	(^{19}F)	(^{7}Li)	(^{19}F + ^{7}Li)
LiBF$_4$	3.4	4.0	1.2	5.2
LiN(SO$_2$CF$_3$)$_2$	6.3	7.1	0.90	8.0
LiAl[OCH(CF$_3$)$_2$]$_4$	6.6	8.0	1.0	9.0

salt concentration in the polyether electrolytes is increased, concentration of the charge carriers increases. Such an increase, on the other hand, also causes diminution of the ionic carrier mobility, which is synchronized with segmental motion of the polyether. These facts result in a maximum for each of the polymer electrolytes in the ionic conductivity versus salt concentration, and it is not surprising that the optimum concentration at which the maximum is attained differs for the different polymer electrolytes. The optimum concentration for the maximum in the polyether electrolytes follows the order Al[OCH(CF$_3$)$_2$]$_4^-$ > N(SO$_2$CF$_3$)$_2^-$ > BF$_4^-$. This is in good agreement with the order of the magnitude of the T_g for the electrolytes with increasing salt concentration, as shown in Figure 5. It is interesting that the increase in the T_g for LiAl-[OCH(CF$_3$)$_2$]$_4$ electrolytes against salt concentration is less pronounced as compared to other systems. The difference in the extent of increase in the T_g for polyether electrolytes containing lithium salts with increase in salt concentration has been well documented. On one hand, for lithium salts with a strong electron-donating anion such as LiCl or LiBr, a moderate increase in the T_g is evident.[31] On the other hand, lithium salts with anions having relatively lower ability to donate electrons like LiBF$_4$ and LiClO$_4$ exhibit pronounced dependence of the T_g on the salt concentrations in polyethers. When incorporated in polymer electrolytes, LiN(SO$_2$CF$_3$)$_2$ moderately increases the T_g, compared to other common lithium salts. This has been explained in terms of the flexibility of N(SO$_2$CF$_3$)$_2^-$ resulting from the flexible S−N−S bond, and the negative charge delocalization induced by the strongly electron-withdrawing −SO$_2$CF$_3$ groups on the nitrogen atom, which weakens the electron donor ability and the interaction with the matrix polyether chain.[16] For the present aluminate salt, the plasticizing effect reflected by the flexible structure of the substituents in Al[OCH(CF$_3$)$_2$]$_4^-$ and weak coordination ability of the anion may give rise to comparatively low T_g of the polyether electrolytes.

Ionic Diffusion Mechanisms in Polyether Electrolytes. To have a microscopic understanding of the ionic transport behavior, PGSE-NMR measurements were carried out. Table 3 lists the self-diffusion coefficients of the lithium ion, anion, and a simple summation of the lithium ion and anion at 80 °C for the P(EO/MEEGE)-based polymer electrolytes containing LiBF$_4$, LiN(SO$_2$CF$_3$)$_2$, and LiAl[OCH(CF$_3$)$_2$]$_4$ at [Li]/[O] = 0.10. The apparent degree of dissociation estimated by using the Nernst−Einstein equation for the polyether electrolytes is

surprisingly high at ca. 0.7−0.85. The incompatibility between the low self-diffusion coefficients of about 10^{-8}–10^{-7} cm^2 s^{-1} and the reasonably high ionic conductivities up to 10^{-4} S cm^{-1} also imply that the lithium salts achieve a high degree of dissociation in the polyether matrixes.

The lithium diffusion coefficients exhibit approximately the same values despite a large difference in the T_g of the polyether electrolytes. The strong ion−dipole interaction of the lithium ion with the polyether may predominantly provide lithium-hopping motion induced by the polyether segmental motion. However, it is evident in this study that the correlation time of ^{1}H of the polyether as determined by the T_1 measurements is shorter than that of ^{7}Li in the polymer electrolytes (data not shown), which coincides with the past observations.[23−25] Thus, the difference in the T_g might not be directly reflected in lithium diffusivity in the NMR time scale. Another explanation for the similar lithium diffusivity would be simply based on the fact that the measuring temperature is far higher than the T_g so that the difference in the diffusivity, depending on the incorporated salt species, is made ambiguous. On the contrary, the anions diffuse much faster than the lithium ion, and large differences in the anionic diffusion coefficients are observed. The anionic diffusion coefficient follows the distinct order of Al[OCH(CF$_3$)$_2$]$_4^-$ > N(SO$_2$CF$_3$)$_2^-$ > BF$_4^-$, which agrees well with the order of ionic conductivity in each of the polyether electrolytes at the same concentration. This is a clear indication of the fact that ionic conductivities obtained here are dominated by the anionic diffusivities. The order of the relative anionic volume approximated from their crystallographic volume does not match with the order of anionic diffusivity. It is well known that the diffusion of small particles in media such as amorphous polymers and glass-forming liquids at temperatures above the T_g is expressed by the following equation:

$$D = gdv \exp\left(-\frac{\gamma V^*}{V_f}\right) \qquad (3)$$

where $g \approx 1/6$, d is the distance through which the particles are transported, v is the velocity of the particle, γ is a factor to allow for overlap of free volume, V^* is the critical volume required for migration of the particle, and V_f is the free volume of the media.[32] The γV^* in the exponential term is generally assumed to equal the size of diffusive particles. Equation 3 suggests that the diffusivity is mainly influenced by the exponential factor, and the ratio of the size of the diffusive particles and the free volume determines the diffusivity. In other words, even if a diffusive particle size is large, a high diffusion coefficient will be likely if the free volume of the system is significantly large. Since the LiAl[OCH(CF$_3$)$_2$]$_4$ electrolyte has a quite low T_g, the higher anionic diffusivity might be explained even though the size is large.

Polyether Electrolytes/Lithium Electrode Interface. Interfacial stability and charge-transfer resistance between metallic

Design of Polymer Electrolytes

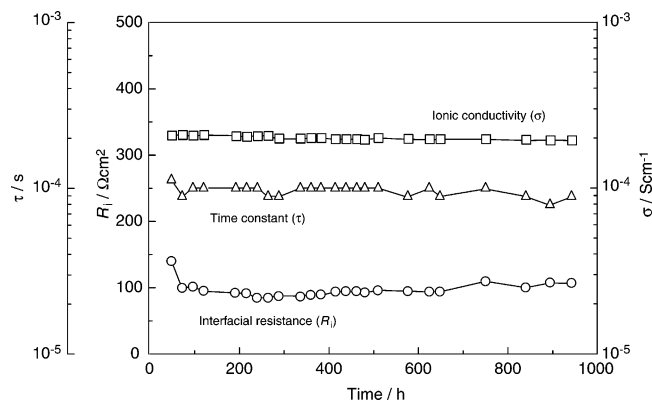*J. Phys. Chem. B, Vol. 108, No. 32, 2004* **12001**

Figure 6. Time dependence of interfacial resistance (circle) and time constant (triangle) for the interface between polymer electrolytes based on P(EO/MEEGE) = 95/5 containing LiAl[OCH(CF$_3$)$_2$]$_4$ ([Li]/[O] = 0.06) and lithium electrode and bulk ionic conductivity (square) at 60 °C.
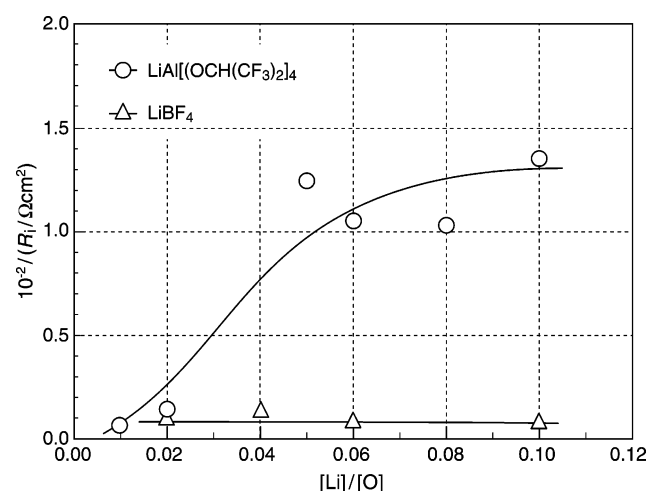

Figure 7. Reciprocal of interfacial resistance for polymer electrolytes based on P(EO/MEEGE) = 95/5 containing LiBF$_4$ and LiAl[OCH-(CF$_3$)$_2$]$_4$ as a function of salt concentration.

lithium and the polyether electrolytes containing LiAl[OCH-(CF$_3$)$_2$]$_4$ have been investigated by the complex impedance method. Figure 6 shows time dependence of the interfacial resistance (R_i) and the time constant (τ) for the interface between the P(EO/MEEGE)-based polymer electrolyte containing LiAl-[OCH(CF$_3$)$_2$]$_4$ ([Li]/[O] = 0.06) and lithium electrode and the bulk ionic conductivity (σ) at 60 °C. The τ has been estimated from a low frequency semicircle of an impedance spectrum of the symmetrical cell assuming that its equivalent circuit could be simply expressed by parallel combination of the interfacial resistance, R_i, and the double layer capacitance. It is obvious here that the polyether electrolyte interface remains stable for a considerably long period. The time dependence of the electrochemical interface between network polyether electrolytes and the metallic lithium electrode by impedance and X-ray photoelectron spectroscopy (XPS) was reported earlier.[33] The R_i for the network polyether electrolytes containing LiN(SO$_2$-CF$_3$)$_2$ also shows a constant value, whereas in LiBF$_4$ an increase in the R_i over the period of time is observed. The results shown in Figure 6 indicate that the anion, Al[OCH(CF$_3$)$_2$]$_4{}^-$, is stable with highly reactive metallic lithium.

Figure 7 shows the reciprocal of the R_i for the polyether electrolytes containing LiBF$_4$ and LiAl[OCH(CF$_3$)$_2$]$_4$ plotted against the salt concentration. The change in the R_i values depends on the nature of lithium salts. In LiBF$_4$, the reciprocal of the R_i shows lower values compared to those for LiAl[OCH-
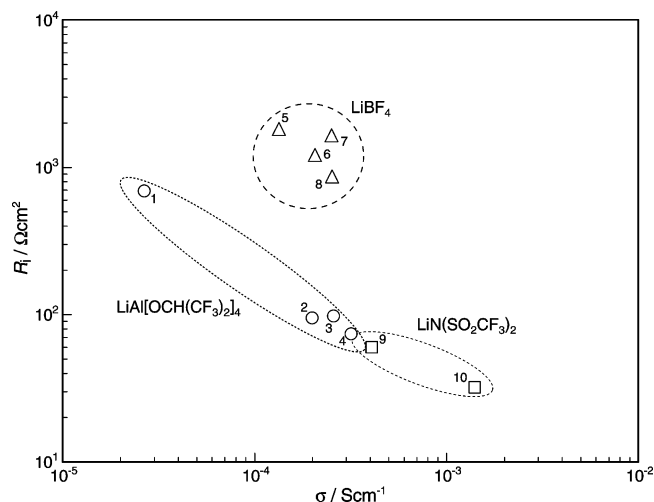

Figure 8. Relationship between bulk ionic conductivity and interfacial resistance for polymer electrolytes based on P(EO/MEEGE) = 95/5 containing LiAl[OCH(CF$_3$)$_2$]$_4$ at [Li]/[O] = 0.02 (**1**), 0.06 (**2**), 0.08 (**3**), and 0.10 (**4**) and LiBF$_4$ at [Li]/[O] = 0.02 (**5**), 0.04 (**6**), 0.06 (**7**), and 0.10 (**8**), polymer electrolytes based on P(EO/MEEGE) = 91/9 containing LiN(SO$_2$CF$_3$)$_2$ at [Li]/[O] = 0.06 (**9**), polymer electrolytes based on P(EO/MEEGE) = 73/27 containing LiN(SO$_2$CF$_3$)$_2$ at [Li]/[O] = 0.06 (**10**) at 60 °C. The dashed lines are guides for the eyes.

(CF$_3$)$_2$]$_4$ and is nearly independent of the salt concentration. The R_i of LiBF$_4$ is ascribed to the highly resistive passivation layer. In LiAl[OCH(CF$_3$)$_2$]$_4$, on the other hand, the inverse of the R_i increases with increase in the salt concentration. If the R_i is assumed to be the charge-transfer resistance (R_{ct}), the reciprocal of the R_i becomes proportional to the exchange current density and can be expressed by the Butler−Volmer equation approximated at low overpotential. The exchange current density is proportional to the activity of a redox-active species, that is, the lithium ion in the present case. For LiAl[OCH(CF$_3$)$_2$]$_4$, the R_i in Figure 7 seems to correspond to the R_{ct}, and the decrease in the R_{ct} can be attributed to an increase in the lithium ionic activity. In general, an increase in salt concentration brings about an increase in ionic association of an electrolyte, mainly because of the enhancement of ion−ion interaction. However, the polyether electrolytes containing LiAl[OCH(CF$_3$)$_2$]$_4$ exhibit the lowest R_{ct} at a relatively high salt concentration of [Li]/[O] = 0.10. Thus, the observation clearly demonstrates that the electrochemical reaction at the lithium/polyether electrolyte solid−solid interface can be controlled by the bulk property of polyether electrolytes.

Finally, the relationship between the ionic conductivity and the interfacial resistance for several P(EO/MEEGE)-based polymer electrolytes containing LiBF$_4$, LiN(SO$_2$CF$_3$)$_2$, and LiAl-[OCH(CF$_3$)$_2$]$_4$ at 60 °C, on the basis of the results of the current and previous studies, are summarized in Figure 8. It can be instantly recognized that the relationship can be discriminated, depending on the dissolved lithium salt, as depicted in Figure 8 by the dashed lines. While no relationship is found for the highly passivative LiBF$_4$ electrolytes (no. 5−8), in the case of lithium salts that form stable lithium/electrolyte interfaces such as LiN(SO$_2$CF$_3$)$_2$ and LiAl[OCH(CF$_3$)$_2$]$_4$, the increase in the bulk ionic conductivity directly gives rise to the decrease in the interfacial resistance. The interfacial resistance decrease, that is, the bulk conductivity increase, is caused not only by the salt concentration increase, as in LiAl[OCH(CF$_3$)$_2$]$_4$ (no. 1−4), but also by the increase in the MEEGE composition in the copolymers (no. 9, 10), which introduces highly mobile ion-coordinating side chains.[8b] Although the charge-transfer resistance at a high lithium salt concentration is lowered, the ionic

conductivity for common lithium salts passes through a maximum and tends to decrease because of significant increase in the T_g. The conductivity maximum appears at much higher salt concentration for the polymer electrolytes containing LiAl[OCH-$(CF_3)_2]_4$. Thus, the lithium salt, LiAl[OCH(CF$_3$)$_2$]$_4$, a lithium salt of a weakly coordinating anion, allows in the polyether not only high ionic conductivity but also low interfacial resistance.

Conclusion

To achieve a polymer electrolyte with high ionic conductivity and fast charge-transfer reaction at the polymer electrolyte/electrode interface, a novel lithium salt of a weakly coordinating anion, LiAl[OCH(CF$_3$)$_2$]$_4$, has been incorporated in a polyether. The salt, in terms of its characteristics of low T_g and anionic weak coordinating ability, exhibits much smaller increase in the T_g with increasing concentration in the polyether electrolytes, compared to LiN(SO$_2$CF$_3$)$_2$ and LiBF$_4$. This enables the polymer electrolytes to incorporate the salt up to a high concentration without loss of the conductivity. The lithium/LiAl[OCH-$(CF_3)_2]_4$−polyether electrolyte interface is statically stable, and the R_i, dominated by the charge-transfer resistance, decreases with increased salt concentration, which is due to high lithium ionic activity in the bulk. We have already proposed a strategy to enhance the charge-transfer reaction at the interface; an increase in the MEEGE composition in the P(EO/MEEGE) copolymers, that is, the introduction of a highly mobile ion-coordinating side chain, induces a decrease in the charge-transfer resistance, in addition to an increase in the bulk ionic conductivity.[8b] In this study, the high ionic conductivity and low charge-transfer resistance are compatible with the lithium salt concentration. The introduction of a lithium salt of a weakly coordinating anion can be a new concept for the design of novel polymer electrolytes.

References and Notes

(1) *Polymer Electrolyte Reviews 1 and 2*; MacCallum, J. R., Vincent, C. A., Eds.; Elsevier: London, 1987 and 1989.

(2) Gray, F. M. *Solid Polymer Electrolytes*; VCH Publishers: New York, 1991.

(3) *Application of Electroactive Polymers*; Scrosati, B., Ed.; Chapman & Hall: London, 1993.

(4) Blonsky, P. M.; Shriver, D. F.; Austin, P. E.; Allcock, H. R. *J. Am. Chem. Soc.* **1984**, *106*, 6845. (b) Allcock, H. R.; O'Conner, S. J. M.; Olimeijer, D. L.; Napierala, M. E.; Cameron, C. G. *Macromolecules* **1996**, *29*, 7544.

(5) (a) Spindler, R.; Shriver, D. F. *Macromolecules* **1988**, *21*, 648. (b) Spindler, R.; Shriver, D. F. *J. Am. Chem. Soc.* **1988**, *110*, 3036.

(6) Hooper, R.; Lyons, L. J.; Mapes, M. K.; Schumacher, D.; Moline, D. A.; West, R. *Macromolecules* **2001**, *34*, 931.

(7) (a) Nishomoto, A.; Agehara, K.; Furuya, N.; Watanabe, T.; Watanabe, M. *Macromolecules* **1999**, *32*, 1541. (b) Watanabe, M.; Hirakimoto, T.; Mutoh, S.; Nishimoto, A. T. *Solid State Ionics* **2002**, *148*, 399.

(8) (a) Nishimoto, A.; Watanabe, M.; Ikeda, Y.; Kohjiya, S. *Electrochim. Acta* **1988**, *43*, 1177. (b) Watanabe, M.; Endo, T.; Nishimoto, A.; Miura, K.; Yanagida, M. *J. Power Sources* **1999**, *81−82*, 786.

(9) Angell, C. A.; Liu, C.; Sanchez, E. *Nature* **1993**, *362*, 137.

(10) Watanabe, M.; Yamada, S.; Sanui, K.; Ogata, N. *J. Chem. Soc. Chem. Commun.* **1993**, 929.

(11) Noda, A.; Watanabe, M. *Electrochim. Acta* **2000**, *45*, 1265.

(12) (a) Seki, S.; Kaneko, T.; Tokuda, H.; Noda, A.; Susan, M. A. B. H.; Watanabe, M. to be submitted. (b) Susan, M. A. B. H.; Kaneko, T.; Noda, A.; Watanabe, M., to be submitted.

(13) Ue, M. *J. Electrochem. Soc.* **1994**, *141*, 3336.

(14) Aihara, Y.; Bando, T.; Nakagawa, H.; Yoshida, H.; Hayamizu, K.; Akiba, E.; Price, W. S. *J. Electrochem. Soc.* **2004**, *151*, A119.

(15) (a) Ue, M.; Takeda, M.; Takehara, M.; Mori, S. *J. Electrochem. Soc.* **1997**, *144*, 2684. (b) Ue, M.; Murakami, A.; Nakamura, S. *J. Electrochem. Soc.* **2002**, *149*, A1572.

(16) (a) Armand, M.; Gorecki, W.; Andréani, R. *Second International Meeting on Polymer Electrolytes*; Scrosati, B., Ed.; Elsevier: New York, 1990; p 91. (b) Vallée, A.; Besner, S.; Prud'homme, J. *Electrochim. Acta* **1992**, *37*, 1579.

(17) (a) Strauss, S. H. *Chem. Rev.* **1993**, *93*, 927. (b) Lupinetti, A. J.; Strauss, S. H. *Chemtracts-Inorg. Chem.* **1998**, *11*, 565.

(18) Reed, C. A. *Acc. Chem. Res.* **1998**, *31*, 133.

(19) Tokuda, H.; Watanabe, M. *Electrochim. Acta* **2003**, *46*, 2085.

(20) Ivanov, S. V.; Miller, S. M.; Anderson, O. P.; Solntsev, K. A.; Strauss, S. H. *J. Am. Chem. Soc. Commun.* **2003**, *125*, 4694.

(21) Kono, M.; Hayashi, E.; Watanabe, M. *J. Electrochem. Soc.* **1998**, *145*, 1521.

(22) Price, W. S.; Hayamizu, K.; Ide, H.; Arata, Y. *J. Magn. Reson.* **1999**, *139*, 205.

(23) Hayamizu, K.; Aihara, Y.; Price, W. S. *J. Chem. Phys.* **2000**, *113*, 4785.

(24) Hayamizu, K.; Aihara, Y.; Price, W. S. *Electrochim. Acta* **2001**, *46*, 1475.

(25) Hayamizu, K.; Akiba, E.; Bando, T.; Aihara, Y.; Price, W. S. *Macromolecules* **2003**, *36*, 2785.

(26) Stejskal, E. O. *J. Chem. Phys.* **1965**, *43*, 3597.

(27) Ivanova, S. M.; Nolan, B. G.; Kobayashi, Y.; Miller, S. M.; Anderson, O. P.; Strauss, S. H. *Chem. Eur. J.* **2001**, *7*, 503.

(28) Hayamizu, K.; Aihara, Y.; Arai, S.; Martinez, C. G. *J. Phys. Chem. B* **1999**, *103*, 519.

(29) Xu, W.; Angell, C. A. *Electrochem. Solid-State Lett.* **2000**, *3*, 366.

(30) Webber, A. *J. Electrochem. Soc.* **1991**, *138*, 2586.

(31) Watanabe, M.; Itoh, M.; Sanui, K.; Ogata, N. *Macromolecules* **1987**, *20*, 569.

(32) Cohen, M. H.; Turnbull, D. *J. Chem. Phys.* **1959**, *31*, 1164.

(33) Iqbal, I.; Noda, A.; Nishimoto, A.; Watanabe, M. *Electrochim. Acta* **2001**, *46*, 1595.

(34) Yoshida, H.; Mizutani, M. *Denki Kagaku* **1994**, *62*, 1023.

(35) *Organic Solvents*, 3rd ed.; Riddick, J. A., Bunger, W. B., Sakano, T. K., Eds.; John Wiley & Sons: New York, 1970.

(36) *Handbook of Chemistry and Physics*, 80th ed.; Lide, D. R., Ed.; CRC Press: Boca Raton, FL, 1999−2000.

(37) Izutsu, K. *Electrochemistry of Non-Aqueous Solutions*; Baifukan: Tokyo, 1995.